PERGAMON

Journal of Structural Geology 22 (2000) 505–518

JOURNAL OF STRUCTURAL GEOLOGY

www.elsevier.nl/locate/jstrugeo

Evaluation of multiple emplacement mechanisms: the Huichizi granite pluton, Qinling orogenic belt, central China

Tao Wang[a, b,*], Xiaxia Wang[c], Wuping Li[c]

[a]*Department of Geology, Peking University, Beijing, 100871, People's Republic of China*
[b]*Department of Geology, Northwest University, Xi'an, 710054, People's Republic of China*
[c]*Department of Natural Resources, Xi'an Engineering University, Xi'an 710054, People's Republic of China*

Received 20 January 1999; accepted 2 November 1999

Abstract

Three end-member granite emplacement mechanisms, host-rock ductile shortening (HRDS), host-rock rigid displacement (HRRD) and magmatic absorption (MA), are identified in this study of the Huichizi pluton. The internal fabrics are mainly flattening types ($\nu = 0.4$–0.9) and strain is high ($Es = 1.0$–0.6) near the boundaries and low ($Es = 0.7$–0.30) toward the central parts of the pluton. In the 1.5-km-wide contact aureole, extension (ε) is measured in syn-emplacement deformed veins and the calculated average shortening normal to the sides and tips of the pluton are 1.14 km and 0.74 km, respectively. From this we conclude that the HRDS produced only about 20% space for the present volume of the pluton; the regional HRRD, derived from the uplift by about 8 km of the Qinling group in a flower structure, contributed $19 \sim 32\%$ space. MS, including stoping and material transfer processes, yielded another 37% space. Of this, stoping contributed a minimum of 1% space, estimated from the surface area of 2.8 km^2 covered by xenoliths. Transfer processes provided about 36% of the needed space, deduced from the average 64/36 ratio of hybridization of mantle-derived to crustal- (Qinling group) derived magma. The three mechanisms may act nearly simultaneously as a multiple emplacement mechanism; this situation may apply to many other plutons as well.

1. Introduction

Granite plutons are an important component of the crust and occupy a substantial crustal volume, especially in orogenic belts. The way in which plutons are emplaced remains a challenging and controversial problem in geology. The chief problem is how space is made for the plutons. Several mechanisms have been proposed (see reviews in Pitcher, 1979; Castro, 1987; Hutton, 1988a; Atherton, 1993; Paterson and Fowler, 1993a). Some authors emphasized forceful emplacement mechanisms of magma, such as ballooning (e.g. Sylvester et al., 1978; Bateman, 1984, 1985, 1989; Mahmood, 1985; Marre, 1986; Castro, 1987; Courrioux, 1987; Ramsay, 1989; Brun et al., 1991) and diapirism (e.g. Van den Eeckhout et al., 1986; Weinberg and Podladchikov, 1994; Weinberg, 1995). Many researchers have pointed to the syntectonic nature of igneous activity (Pitcher, 1979; Hutton, 1982, 1988a, b; Karlstrom et al., 1993) and emphasized the role of local tensional or potentially dilational sites in shear zones in settings such as extension, transtension and transpression (e.g. Guineberteau et al., 1987; Hutton, 1988a, b, 1992, 1997; Hutton et al., 1990; Glazner, 1991; Saleeby, 1991; Clemens and Mawer, 1992; D'Lemos et al., 1992; Hutton and Reavy, 1992; Petford and Atherton, 1992; Brown, 1994; Tobisch and Cruden, 1995; Karlstrom et al., 1993). These mechanisms were generally grouped into forceful mechanisms and permissive mechanisms. Recent studies, however, indicate that single-mechanism models all have shortcomings and terms such as 'forceful' and

* Corresponding author.
E-mail address: taowang@pub.xa-online.sn.cn (T. Wang).

0191-8141/00/$ - see front matter
PII: S0191-8141(99)00169-8

'permissive' should be discarded (Paterson and Fowler, 1993a; Paterson and Vernon, 1995). Forceful expansion mechanisms such as ballooning cannot make enough space for plutons (Paterson and Fowler, 1993a; Godin, 1994; Paterson and Vernon, 1995; Castro and Fernández, 1998). Models based on local extension derived from shear zones are difficult to apply to elliptical plutons (Paterson and Fowler, 1993b; Yoshinobu et al., 1995). Paterson and Fowler (1993a) have proposed multiple near-field and far-field material transfer processes (MTPs) and suggested that workers need to look for multiple emplacement mechanisms rather than a single mechanism. Some studies have indeed recognized multiple mechanisms during pluton emplacement, for example, stoping and other brittle mechanisms (Law et al., 1992); stoping, roof uplift, reactivation of country rock cleavage and an actively forming antiform (Davis, 1993); roof uplift and surface erosion (Godin, 1994); ductile flow, stoping and minor regional faulting (Vernon and Paterson, 1993); stoping, subsequent volume loss and ductile flow (John and Blundy, 1993). More recently, McNulty et al. (1996) and Paterson and Miller (1998) not only recognized multiple mechanisms but also estimated the contribution of some mechanisms. However, it is still not clear how many and what kinds of mechanisms are involved for certain plutons, how much space is provided by each of them.

This paper documents an example where multiple emplacement mechanisms are recognized and can be grouped into three end-member mechanisms, i.e. host-rock ductile shortening, host-rock rigid displacement and magmatic absorption. We infer that the multiple

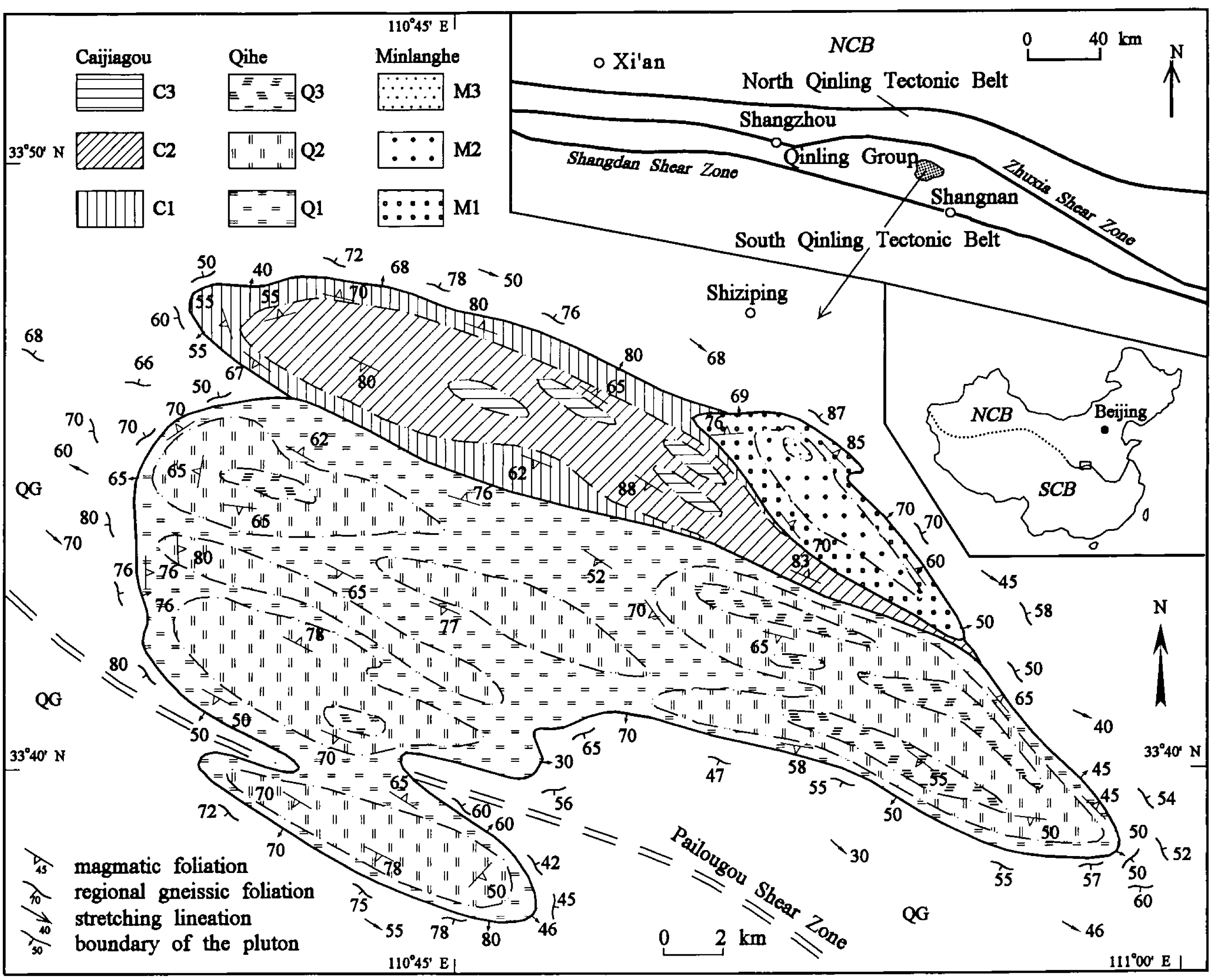

Fig. 1. Geological sketch map of the Huichizi pluton and its regional geological setting. C1, C2, C3, Q1, Q2 Q3 and M1, M2, M3 are the first, second and third unit of Caijiagou (C), Qihe (Q) and Minglanghe sequence (M), respectively; NCB, North China Block; SCB, South China Block.

emplacement mechanisms may be effective for many plutons in nature.

2. Regional geological setting

The Huichizi granite pluton occurs in the Qinling group located at the center of the Qinling orogenic belt, one of the main orogenic belts in East Asia separating the North China Block from the South China Block, a composite continental orogen that evolved under several tectonic regimes and mainly formed from the Palaeozoic to the Early Mesozoic (Zhang et al., 1989, 1995a; Fig. 1). The Qinling group is assumed to form the old Precambrian crystalline basement of the belt and is predominately composed of metasedimentary and metavolcanic rocks in amphibolite facies, including various felsic schists, gneisses, quartzites, marbles and amphibolites (Zhang et al., 1988, 1995b; You et al., 1990; Wang et al., 1997a). These rocks were originally deposited in the early Proterozoic and later underwent two tectonothermal events. In the Late Proterozoic, the rocks were subducted to a depth of about 30 km, forming the metamorphic terrane, were then reworked during uplift between 457 and 332 Ma, accompanied by granite intrusion (You and Suo, 1991; Wang et al., 1997a, b). The group lies at the boundary area between the North Qinling Tectonic Belt and the South Qinling Tectonic Belt and is distributed in the form of an elongated lens among Paleozoic terranes (Fig. 1).

The Huichizi granitoid pluton, a part of the magmatic arc (Lerch et al., 1995), is the largest pluton in the center of the Qinling orogenic belt. Based on the 1:50 000 scale regional geological mapping (Wang and Li, 1996), the pluton is divided into three sequences from older to younger: Caijiagou (C), Qihe (Q) and Minglanghe (M). Every sequence is composed of three units (Li and Wang, 1995a). The Caijiagou sequence is composed of medium- to fine-grained tonalite (C1), medium- to fine-grained granodiorite (C2) and medium-grained granodiorite (C3); the Qihe sequence is composed of medium- to fine-grained granodiorite (Q1), K-feldspar phenocryst bearing (5%) granodiorite (Q2) and K-feldspar phenocryst bearing (8%) monzonitic granite (Q3); the Minglanghe sequence is composed of K-feldspar phenocryst bearing (12%) granodiorite (M1), K-feldspar bearing (15%) monzonitic granite (M2) and K-feldspar phenocryst bearing (20%) monzonitic granite (M3). An age of 437 Ma (single-zircon evaporation Pb–Pb method) has been obtained for the earliest unit of the Caijiagou sequence (Wang and Li, 1996) and 382 Ma (Rb–Sr) for the Minglanghe sequence (Shang and Yan, 1988). In addition, a large number of 381–366 Ma (K–Ar) ages were determined for granitic pegmatites (Chen et al., 1993), genetically related to the pluton and intruded into it as veins. This seems to imply that the intrusion and cooling time span for the magma sequences may be relatively long.

Recent studies show that the pluton is a hybrid granite, i.e. H-type (Castro et al., 1991), formed from hybrid magmas derived from the Qinling group and from the deeper basic materials derived from the mantle (Zhang et al., 1994; Li and Wang, 1995b).

3. Structural patterns

3.1. Fabrics

Fabrics in plutons are generally developed from magmatic flow to solid-state flow (Paterson et al., 1989; Bouchez et al., 1992; Karlstrom et al., 1993; Miller and Paterson, 1994). In the Huichizi pluton, a preferential mineral orientation defines a magmatic foliation and a weak lineation. The fabric is characterized by a roughly margin-parallel pattern with foliation intensity increasing towards the contact with the host rock (Fig. 1). We identified four development stages for the fabric (Wang et al., 1997c): (1) magmatic flow, marked by the predominant preferential orientation of schlieren layering, euhedral plagioclase and biotite; (2) submagmatic/high-temperature solid-state flow, characterized by inclusions of fine, plastically-deformed plagioclase and quartz grains in K-feldspar megacrysts, indicating that the deformation temperature was at least > 550°C (Miller and Paterson, 1994); (3) moderate–high temperature solid-state flow, marked by plastic deformation (dynamic recrystallization) of the K-feldspar megacrysts, indicating that the temperature was above 600°C (Paterson et al., 1989); (4) moderate–low temperature solid-state deformation, shown by slight fracturing of the feldspars and the presence of fine muscovite along the *C*-planes, indicating that the temperature was much lower (about 330–450°C; Wang et al., 1996).

Detailed observations on a large number of thin sections suggest that particularly the second and third process, also the first are dominant. These processes may belong mainly to syn-emplacement processes, the third stage may represent the transition from a syn-emplacement magma/high-temperature solid flow to syn- (or late-) emplacement regional deformation. The fourth process overprints the other foliations and is characterized by a weak and non-penetrative foliation trending NW–SE, representing the post-emplacement process associated with regional deformation.

3.2. Fabric ellipsoid and fabric pattern

Based on our mapping result, we have systematically

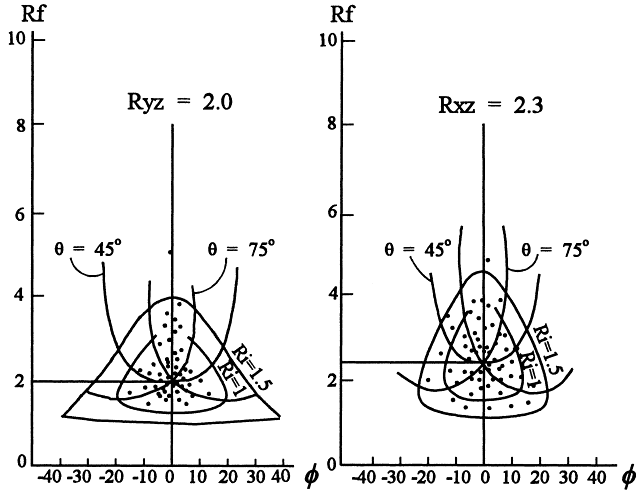

Fig. 2. R_f/ϕ computer diagrams of the quartz markers. The theory curves for $R_i = 1$, $R_i = 1.5$ are shown. The θ curves are for $\theta = 45°$ and 75°, respectively (after Dunnet, 1969; Wang, 1988).

measured the fabric ellipsoid using quartz grains as markers. These quartz grains are generally 2–6 mm in length and show migration recrystallization in thin section. First, sections normal to the foliation and lineation were cut and polished. These are assumed to coincide with XZ, YZ and XY planes of the finite strain ellipsoid. Then, for each section, the two-dimensional shape fabric was determined using an R_f/ϕ (Dunnet, 1969) computer simulation method (Wang, 1988) with 30–50 quartz grain measurements (Fig. 2). Finally, the 3D fabrics were calculated according to the parameters of the 2D fabric ellipses (see Fig. 3). Strain intensities (Es) and fabric types (ν, Lode's parameter) are also calculated by:

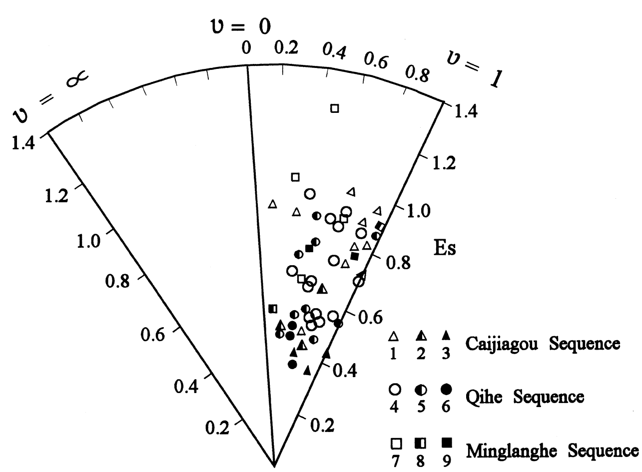

Fig. 3. Hsu diagram (Hsu, 1966) of the measured fabrics (finite strain) of the Huichizi pluton. Es, strain intensity; ν, Lode's parameter (defining ellipsoid shapes). 1, 2 and 3 reflect the first, second and third unit of the Caijiagou sequence; 4, 5, 6 and 7, 8, 9 are those of the Qihe and Minglanghe sequences, respectively.

$$Es = (1/3)\{(\varepsilon_1 - \varepsilon_2)^2 + (\varepsilon_2 - \varepsilon_3)^2 + (\varepsilon_3 - \varepsilon_1)^2\}^{1/2} \quad (1)$$

and

$$\nu = 2((\varepsilon_2 - \varepsilon_1 - \varepsilon_3))/(\varepsilon_1 - \varepsilon_3), \quad (2)$$

respectively; where $\varepsilon_1 = \ln(1 + e_1)$, $\varepsilon_2 = \ln(1 + e_2)$ and $\varepsilon_3 = \ln(1 + e_3)$; $(1 + e_1)$, $(1 + e_2)$ and $(1 + e_3)$ are the lengths of the fabrics (strain) semi-axes and e_1, e_2 and e_3 are the values of principal strain.

Fig. 4 shows the strain data at locations in the pluton. The Es values increase from the center to the marginal areas of the sequences (Fig. 3). This trend also exists within a single unit, e.g. in the Caijjagou sequence (Fig. 5). The values of the Lode parameter (ν) are mostly 0.4–1, showing flattening-type strain. A few of the values are near 0.2, representing slightly linear structures, which are steeply plunging.

The origin of fabric patterns in plutons with high strain at the margins and low strain in the center is difficult to explain (e.g. Paterson et al., 1989, 1998; Paterson and Miller, 1998). It can be a result of: (i) internal igneous processes such as forceful expansion in the fluid state (Guglielmo, 1993), expansion in the subsolid state (Ramsay, 1989), or doming or magma flow (convection) without expansion (Cruden, 1990); (ii) regional tectonic deformation (e.g. Hutton, 1982; Archanjo et al., 1994); or (iii) a combination of these. In the case of the Huichizi pluton, all of these processes may have operated. However, the second, i.e. the syn- and post-emplacement regional tectonic deformation was probably less important, because: (i) the fabrics remain parallel to the boundary at the tips of the pluton where both the foliations and pluton boundary are locally N–S striking and subnormal to the NNW regional structural trend (Figs. 1 and 4); (ii) a number of granodiorite, tonalite and granitic pegmatite veins in the pluton show little or no deformation; (iii) the feldspar and quartz grains in the host-rocks show little dynamic recrystallization. Generally, magmatic fabric patterns in plutons do not provide enough information about ascent or emplacement (Paterson et al., 1998), whereas evaluation of deformation of the host rocks is critical to understanding the processes involved (Fowler and Paterson, 1997).

3.3. Host-rock deformation and syn-emplacement strain

3.3.1. Pre- and post-emplacement host-rock deformation

The pre-emplacement regional deformation, mostly formed in the late Proteozoic, is characterized by regional NW- to WNW-trending schistosity and folds outside the contact aureole of the pluton. Some of the regional small-scale folds such as minor tight folds are found in host-rock xenoliths. After plutonic emplacement, regional ductile deformation was mainly concentrated along ductile shear zones and had little influence

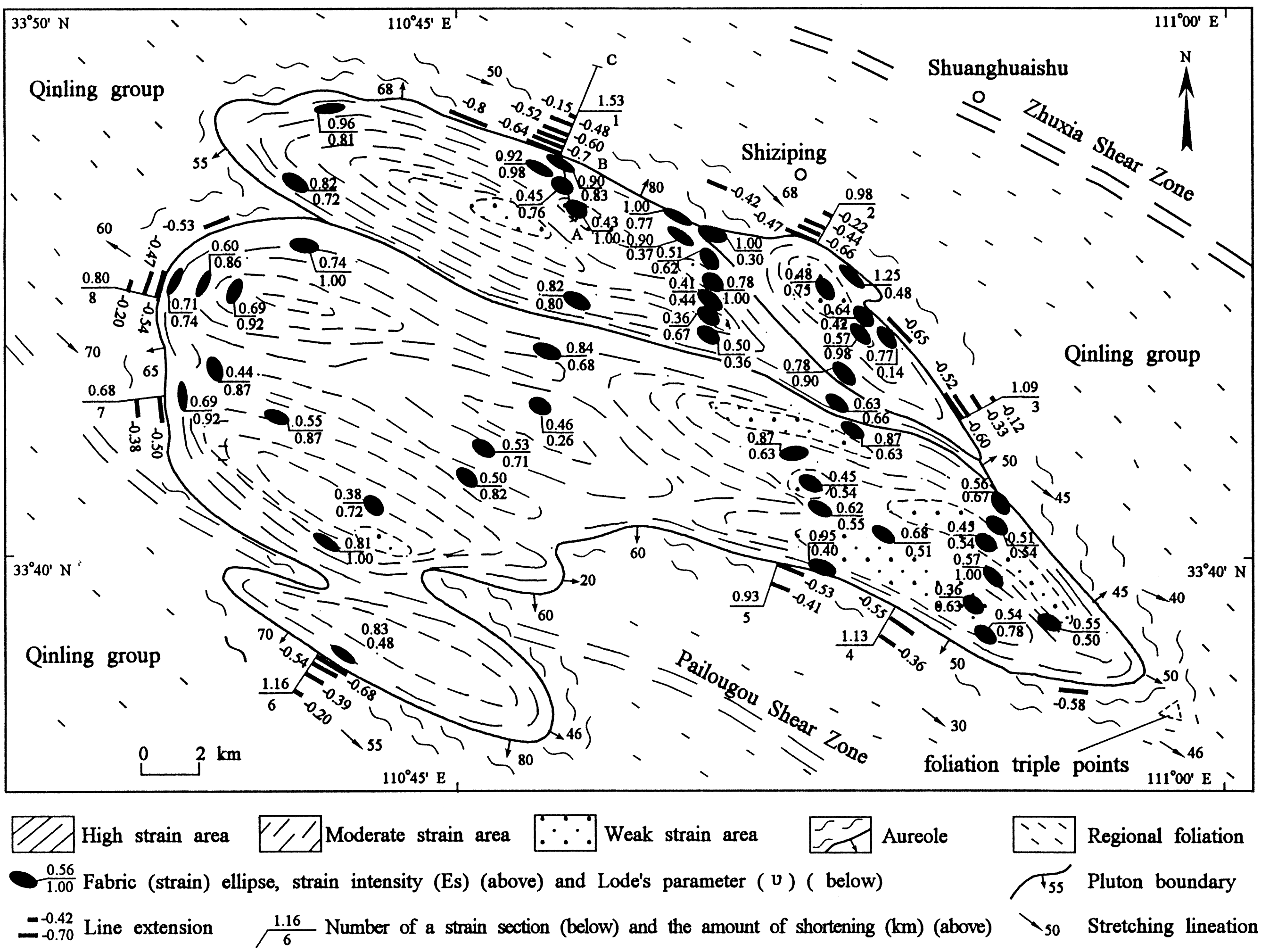

Fig. 4. Structural pattern in the Huichizi pluton.

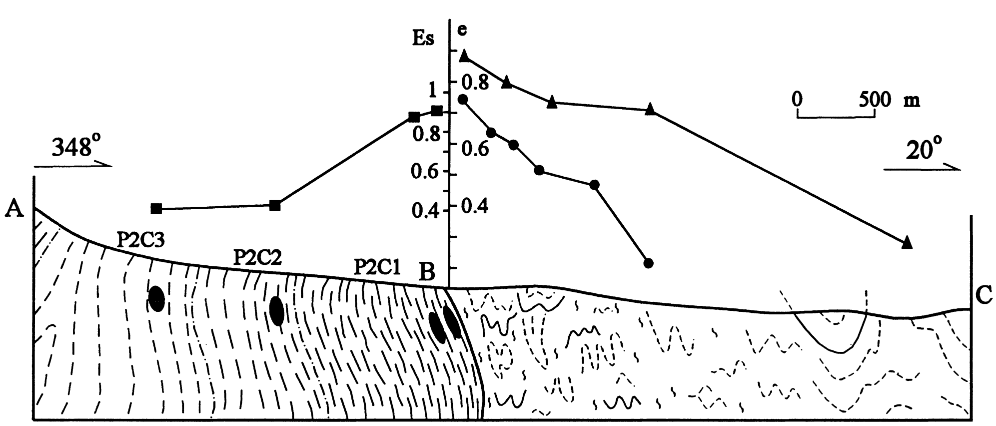

Fig. 5. Strain section (number 1 in Fig. 4) across the pluton boundary. Squares represent strain intensity (Es) measured from deformed quartz markers; Ellipses represent fabric (strain) ellipses nearly in the XZ plane; Circles and triangles represent line extension (e) of folded granitoid veins and gneisses, respectively.

on the early regional structures and the pluton structure (You and Suo, 1991; Wang et al., 1997a).

3.3.2. Syn-emplacement host-rock deformation and strain

Syn-emplacement deformation is marked by the 1.5-km-wide metamorphic/structural aureole of the pluton (Fig. 4). The characteristics of the aureole are:

1. The regional WNW–ESE-trending foliations are rotated toward parallelism with the pluton margin at a distance of 1.0–1.5 km from the pluton; foliation triple points occur at the tips of the pluton. The foliation pattern is similar to an interference pattern between pluton expansion and coaxial tectonic deformation (Guglielmo, 1994). Most mineral lineations, mainly defined by a preferential orientation of quartz, plagioclase and hornblende, plunge steeply, implying that host-rock return flow may have occurred to some degree.
2. Host rocks in the aureole show much more intense deformation than those outside the aureole (Figs. 6 and 7).
3. The degree of metamorphism is higher towards the pluton. In the aureole, the mineral assemblages are typical for middle to upper-amphibolite facies: plagioclase, K-felspar, quartz, biotite, garnet, sillimanite, melt; or plagioclase, K-felspar, quartz, biotite, garnet, melt; or plagioclase, hornblende, biotite. Outside the aureole the mineral assemblages are typical for lower-amphibolite facies: plagioclase, quartz, biotite, garnet, muscovite; or plagioclase, hornblende, biotite, epidotite. Application of the garnet–plagioclase–sillimanite, plagioclase–quartz–biotite–garnet–muscovite barometer and biotite–garnet thermometer indicates that the *P–T* conditions in the aureoles are 0.46–0.61 GPa, 529–847°C; outside the aureoles 0.42–0.58 GPa, 491–510°C (Wang et al., 1995).
4. A large number of granitoid and felsic veins occur in the aureole, mostly about 1–30 cm in width. They are strongly folded (Fig. 7), even at the tips of the pluton, where their fold axial planes are parallel to the pluton boundary and orthogonal to the regional tectonic trending. However, pegmatite veins which cut these veins were weakly deformed (Chen et al., 1993; Wang et al., 1996).

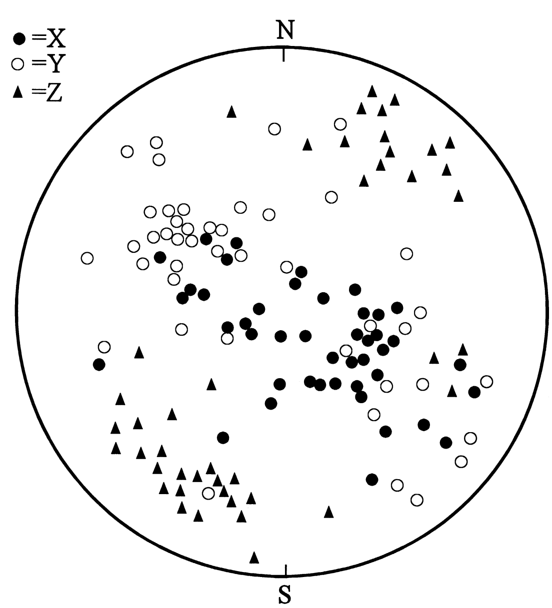

Fig. 6. Lower-hemisphere stereographic projection of poles to the three principal axes of the finite strain ellipsoid. Solid circle, open circle and triangles represent the *X*, *Y* and *Z* axes, respectively.

The observations listed above suggest that the deformation of the veins was nearly simultaneous with pluton emplacement and was mainly caused by these processes. Regional tectonic deformation superimposed on the 'soft' aureole was probably not strong. Hence, we choose these granitoid veins to estimate the syn-emplacement extension in the aureole along radial transects, using Bateman's method. The results (Fig. 4) show that the strain increases towards the boundary (Fig. 7). The average extension from the northeastern and southwestern sides of the pluton is slightly higher (−0.48) than that from the northwestern end (−0.42). The differences may be result of: (i) the slight superposition of the NE–SW regional tectonic contractions on the pluton expansion; or (ii) the differences between the pluton 'expansion' in the sides and ends; or (iii) both of these. In any case, values of −0.48 and −0.42 represent the maximum and minimum host-rock shortening. In addition to these vein folds, some host-rock folds were also measured in the aureole. Their shortening also increases toward the boundary in the aureole (e.g. Fig. 8) and the average is 71%, which can be regarded as the upper limit to the syn-emplacement strain because it may contain pre-emplacement strain of the regional deformation.

4. Evaluation of the three end-member emplacement mechanisms

The following three principle mechanisms are mainly responsible for the emplacement of the Huichizi pluton: host-rock ductile shortening; host-rock rigid displacement; and magmatic absorption.

4.1. Host-rock ductile shortening

The previous sections have shown that host-rock ductile shortening (HRDS) occurred in the emplacement of the Huichizi pluton, which is a mechanism equivalent to forceful expansion (e.g. Bateman, 1984, 1985; Hutton, 1988a; Ramsay, 1989) or ductile return flow in the aureole (Paterson and Miller, 1998; Paterson and Fowler, 1993a). Shortening is commonly estimated according to the width of the aureole and its average strain (e.g. Sylvester et al., 1978; Sanderson and Meneilly, 1981; Bateman, 1985; McNulty, 1996; Paterson and Miller, 1998). Schwerdtner (1995) argued that such calculations might not be correct in a diapiric intrusion because there may also be rigid rotation. In the Huichizi pluton, however, the influence of rigid rotation may be small since the deformation was pervasively ductile.

In this study, we first calculate the shortening (S_i) for a segment width ($D_{i+1} - D_i$) between two strain (ε_i, ε_{i+1}) measurement stations:

$$S_i = (D_{i+1} - D_i)/(1 + (\varepsilon_{i+1} + \varepsilon_i)/2) \quad i = 0, 1, 2, \dots, n \tag{3}$$

where ε_i and ε_{i+1} are the extension (ε) measured from the distances D_i and D_{i+1}, normal to the pluton boundary; $(\varepsilon_{i+1} + \varepsilon_i)/2$ is the average value; n is number of the measurements; $D_0 = 0$; $\varepsilon_0 \approx \varepsilon_i$; $D_n = 1.5$ km (width of the aureole); $\varepsilon_n \approx 0$.

The amount of total shortening (km) of the section (Fig. 4) is now given as:

$$\mathrm{MS} = \sum 2(D_{i+1} + D_i)/(2 + \varepsilon_i + \varepsilon_{i+1}), \tag{4}$$

where MS stands for 'mean shortening'. Taking the example of section 8 (Fig. 4), Eq. (4) gives:

$$\begin{aligned}\mathrm{MS} = {} & 2(0.02 - 0)/(2 - 0.54 - 0.54) + 2(0.5 \\ & - 0.02)/(2 - 0.54 - 0.47) + 2(1 - 0.5)/(2 \\ & - 0.47 - 0.20) + 2(1.5 - 1)/(2 - 0.20 - 0) \\ = {} & 0.80 \text{ km}.\end{aligned} \tag{5}$$

Thus, the average MS of sections 1, 2, 3, 4, 5 and 6 normal to the sides of the pluton is calculated to be 1.14 km (MSs) and the average MS of sections 7 and 8 to the ends of the pluton is 0.74 km (MSe).

If we take the whole Huichizi pluton into consider-

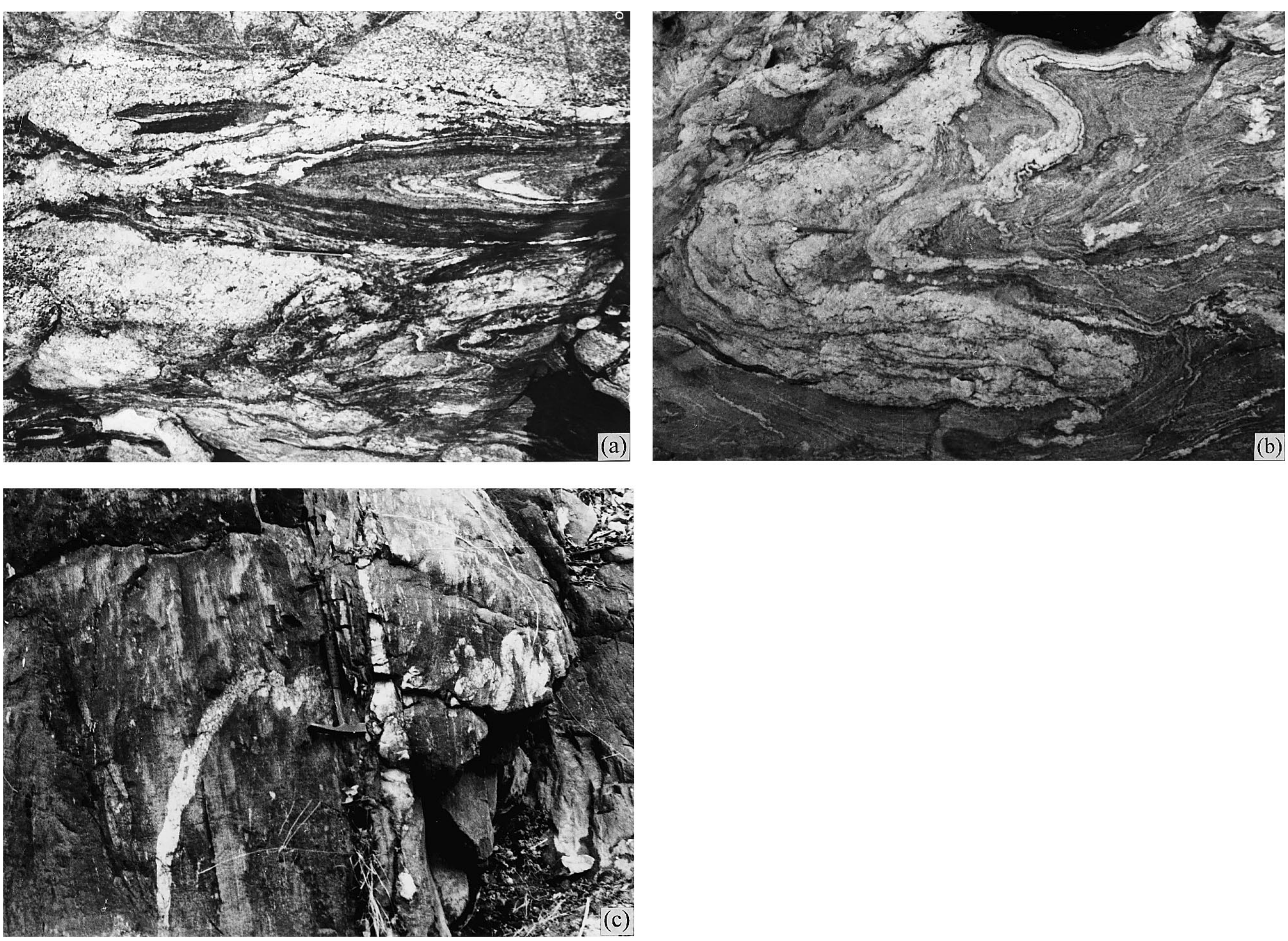

Fig. 7. Syn-emplacement folds in granitoid veins. (a) Isoclinal folds at 5 m from the pluton contact, $\varepsilon = -0.80$. (b) Tight folds at 30 m from the contact, $\varepsilon = -0.75$; (c) Close folds at 1000 m from the contact, $\varepsilon = -0.48$. Fields of view are 112, 128 and 140 cm across, respectively.

ation at the presently exposed level, the pluton has an approximately elliptical shape. The total area of the pluton is therefore:

$$\Delta_f = 15 \times 7 \times \pi = 330\ \text{km}^2. \quad (6)$$

Before the wall rock was shortened, the area of the pluton can be calculated as:

$$\Delta_i = (15 - \text{MSe})(7 - \text{MSs}) \times \pi. \quad (7)$$

Then, the percentage ratio of the shortened area to the present-day area of the pluton is:

$$((\Delta_f - \Delta_i)/\Delta_f) \times 100\%) \approx 20\%. \quad (8)$$

We therefore infer that host-rock ductile shortening may contribute approximately 20% of the necessary emplacement volume of the pluton. Obviously, there must have been other emplacement mechanisms as well.

4.2. Host-rock rigid displacement

The host rock of a pluton can be rigidly displaced by either of two mechanisms:

1. Tectonic processes such as folding, shearing, fracture and regional extension, where the tectonic extension rate is nearly equal to magma influx rate, although mostly not greater, as emphasized by Paterson and Fowler (1993b). The processes may be faster at local conditions in the upper crust (Castro and Fernández, 1998).
2. Expansion of a pluton, where the tectonic extension rate is less than magma influx rate.

Both of these processes are marked by an absence of ductile deformation of the host rocks, which distinguished HRRD from HRDS. Local extension in shear zones is common as a local HRRD mechanism. In the investigated area, however, we see no evidence for these processes.

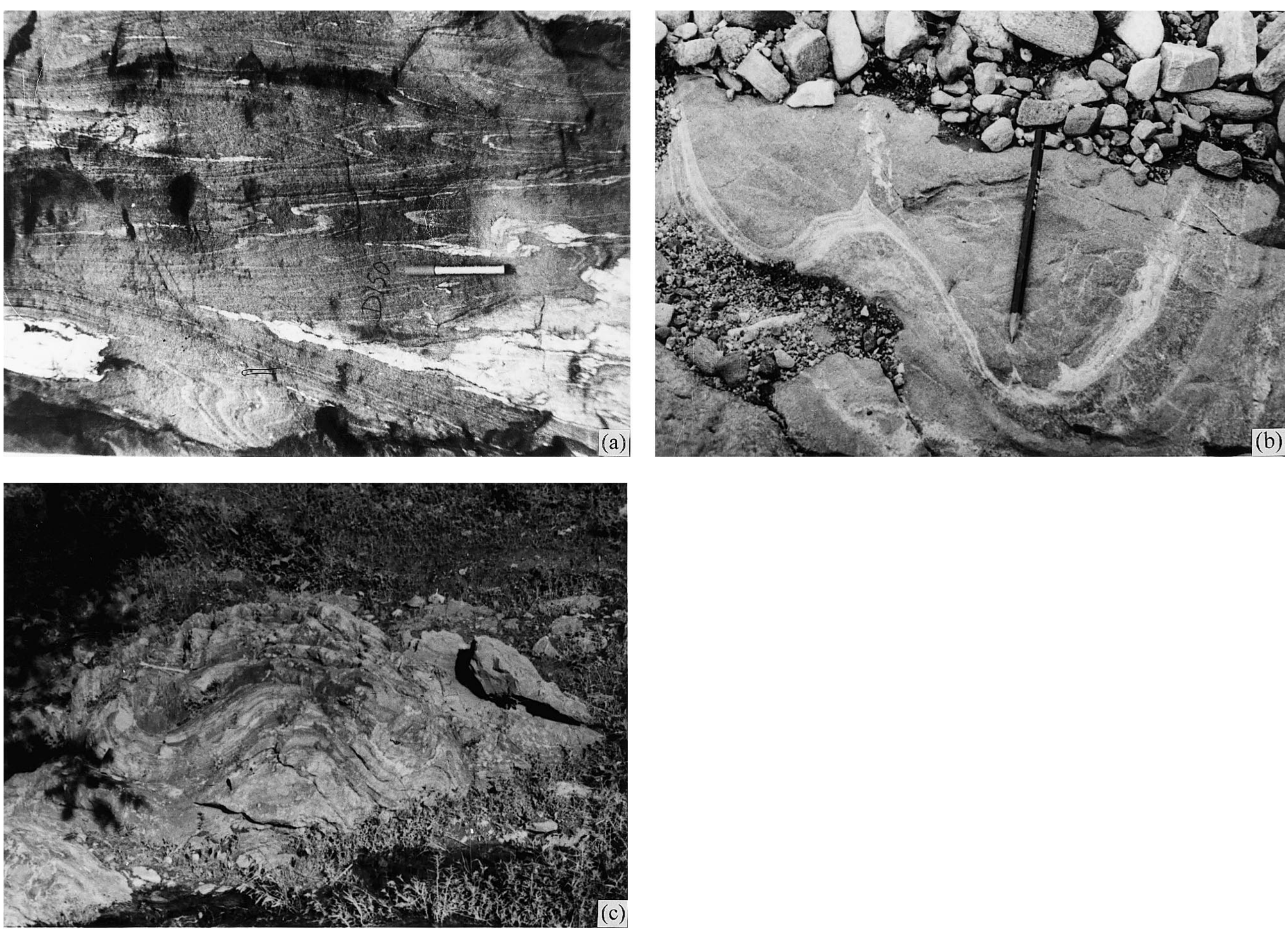

Fig. 8. Photographs of host-rock folds. (a) Isoclinal folds at 35 m from the pluton contact, $\varepsilon = -0.77$. (b) Tight folds at 1100 m from the pluton, $\varepsilon = -0.44$. (c) Closed folds outside the contact aureoles (1600 m from the contact) ε(line extension) $= -0.22$. Fields of view are 105, 64 and 400 cm across, respectively.

From the Lower- to Upper Paleozoic, the Qinling group was uplifted in the form of a flower structure (You and Suo, 1991; Wang et al., 1997b; Fig. 9). You and Suo (1991) established the regional metamorphic *P–T–t* path during the period 425–353 Ma. In this period, pressure decreased from 0.63 to 0.43 GPa, it was therefore concluded that the Qinling group was uplifted over 8 km during this period. Other *P–T–t* path data and comparison of the depth of the Qinling group with that of the strata near the Qinling group (e.g. Erlangping group) further show that the uplift was about 10 km during the period 457–330 Ma (Wang et al., 1997b). As the period 425–353 Ma is more approximate to the time span (437–382 Ma) of the formation of the Huichizi pluton, 8 km is regarded here as the magnitude of uplift during pluton emplacement. During this period, both the boundary shear zones of the Qinling group were thrust. They dip 45° (α) to the south and 60–80° (β) to the north, respectively, as deduced by the geophysical explorations (Yuan, 1991). The tectonic setting of the uplift was two-sided subduction of two finite ocean basins located in the south and north of the island arc that is based on the Qinling group (Zhang et al., 1988). Relative extension could accompany the uplift. This may be similar to extension in the upper plate when subduction rate exceeds convergence rate (Royden, 1993; Grocott et al., 1994) and also similar to 'synconvergent extension' (Thompson et al., 1997, see their fig. 1). The dynamics model may also be likened to extrusion and extension of soft mud between two rigid blocks (Fig. 9; Wang et al., 1997b). The boundary conditions allow the Qinling group to expand during the emplacement or growth of the pluton.

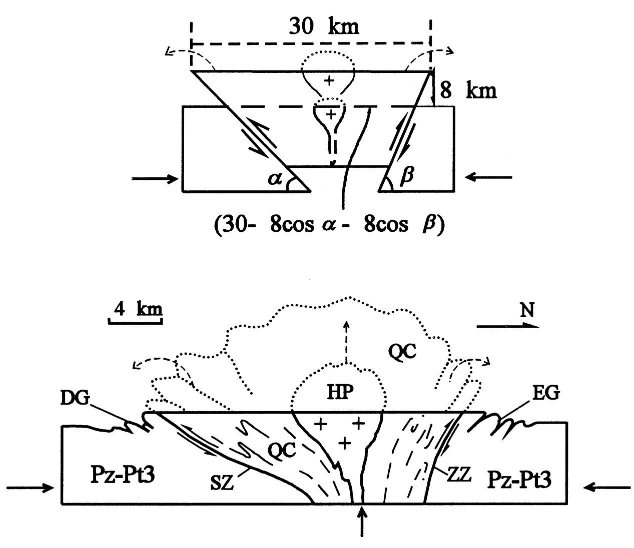

Fig. 9. Uplift of the Qinling complex (QC) in the form of a flower structure and its geometric model. SZ, Shandan zone; ZZ, Zhuxia zone; HP, Huichizi pluton; Pz–Pt3, Paleozoic–late Proterozoic terranes; DG, Danfeng group; EG, Erlangping group; Dotted line and arrow shows the 'syn-extrusion' extension relative to the original form.

In terms of the geometric model (Fig. 9), the percentage of regional horizontal extension is calculated as follows:

$$(1-(\Delta_i/\Delta_f))\times 100\% = [1-(W_i/W)]\times 100\% \qquad (9)$$

where

$$W_i = (Wh\cos\alpha - h\cos\beta), \qquad (10)$$

and where W and h are the exposed width (30 km) and distance (8 km) of the uplifted block, respectively, W_i is the initial W before uplift and, α and β are the angles of the two boundaries of the block, respectively.

Thus the percentage of relative horizontal regional extension or expansion of the Qinling group is about 19–32%. The Huichizi pluton must have fully utilized the potential 19–32% extension space to grow, in addition to making space by ductile shortening of the wall rocks.

4.3. Magmatic absorption

We define the process of magmatic absorption as one in which the magma absorbs its host rock and occupies its space by two processes: mechanical capture (stoping and brecciation) and (or) a material transfer processes such as melting (Marsh, 1982), assimilation and magma hybridization.

We mapped along traverses crossing the pluton at 1-km equidistance and found about 280 xenoliths. They were generally an irregular or lens shape (5 m × 10 m) with an average surface area of 50 m^2 in outcrop. The total area of these xenoliths is therefore approximately 14 000 m^2. If the number of observation lines were increased to let the distance between two lines reach 5 m (average length of the xenoliths), the line density would increase by 200 times. Assuming that the possibility of finding xenoliths was the same as before, the present area of the xenoliths would also increase 200 times. According to this analysis, it can be deduced that the total area of xenoliths in the pluton may be at least about 2.8 km^2. Although this is only about 1% of the total exposed area in the subhorizontal section of the pluton, it demonstrates that mechanical capture (stoping) did occur.

In addition, previous studies show that the pluton is an H-type granite (Castro et al., 1991), which is the result of the hybridization of mantle- and crust- (Qinling group) derived magma (Zhang et al., 1994, 1995; Li and Wang, 1995b; Wang and Li, 1996). The mantle-derived magma is possibly represented by some basic intrusions in the region. The crust- (Qinling group) derived magma is represented by the Piaochi granite pluton (located 8 km away from the northeast boundary of the Huichizi pluton), the composition of which was estimated to be derived for 95% from the Qinling group (Zhang et al., 1996). Zhang et al. (1994) first estimated the mantle:crust ratio (M:C) in the pluton to be about 7:3, based on the analysis of Sm, Nd and Sr isotopes and calculations using the method of Faure (1986). We examined the results using new data on Sm, Nd and Sr ratios and simulated hybridization of the REE in eclogites (Wang and Li, 1996) to constrain the two end-members. We estimated that the average M:C ratio is 64:36 (Li and Wang, 1999, in press). From this, it can be deduced that 36% by volume of the pluton was contributed to by the granitization (and assimilation) of crustal materials, i.e. of the Qinling group, since the difference in density between the two magmas is fairly small compared to the huge volume of magma and can be neglected. Obviously, not all the space (assimilated or melted materials) is transferred from the present-level wall-rocks. Part of it may be derived from the deeper host rock. Space could be transferred by host-rock ductile return flow (Paterson and Fowler, 1993a; McNulty et al., 1996) into the exposed level. The steeply plunging lineation developed in the host-rocks might be the result of such flow. The above calculations establish that magmatic absorption (MA) accounts, in total, for at least 37% of the space involved in the emplacement of the pluton. This reduces the required contribution by other tectonic processes.

5. Discussion

The three mechanisms proposed here, host-rock ductile shortening (HRDS), host-rock rigid displacement (HRRD) and magmatic absorption (MA), are probably the most important mechanisms and may have acted nearly simultaneously to provide space for a pluton.

HRDS is a classical forceful intrusion mechanism. The role of HRDS, however, has often been exaggerated. Generally, shortening cannot contribute more than 40% of the space needed for a pluton (Paterson and Fowler, 1993a). Local HRRDs, such as along faults or shear zones, are usually taken as a space-producing tectonic processes, but they were questioned recently because they do not produce enough space (Paterson and Fowler, 1993b; Yoshinobu et al., 1995). We think that regional HRRD may be of more importance for pluton emplacement. It may exist not only in an extensional tectonic setting, such as extension orogeny, orogenic collapse and oblique convergence, but also in some compressive settings, e.g. synconvergent extension (Thompson et al., 1997). Of the MA processes, stoping appears to be an important emplacement mechanism in some plutons (Fowler et al., 1995; Paterson et al., 1995; Yoshinobu et al., 1995) and occurs at various crustal levels. However, the horizontal sheet shape (Améglio et al., 1997; McCaffrey and Petford, 1997; Siebel et al., 1997; Trzebski et al., 1997; Zulauf et al., 1997) and narrow roots (Améglio et al., 1997; Hecht et al., 1997) of most granite plutons in nature made it difficult to apply generally. Material transfer processes (chemical processes) may be more important, and could be a major mechanism for in-situ and semi-in-situ granites. Recent study shows that such granites are actually generated from hybridization by the mixing of mantle- and crustal-derived magma (e.g. Leek, 1990; Chappell, 1996; Keay et al., 1997; Collins, 1998), i.e. H-type (Castro et al., 1991). Granitization and assimilation of the host rock must therefore have contributed space for granite emplacement. If HRDS and HRRD are regarded as classical forceful and passive mechanisms, MC is a good complement for these two major mechanisms.

In addition to the three end-member mechanisms discussed above, there are certainly other possible mechanisms, but these are generally difficult to recognize and each of them may have contributed less space. For example, in the Huichizi pluton, if the estimations given above are correct, 10–20% of the required space remains unexplained. Volume loss may be one of them, but this could contribute only a little space (e.g. 2%, Paterson et al., 1998). There may be other mechanisms of which we have not found evidence and so further study is needed.

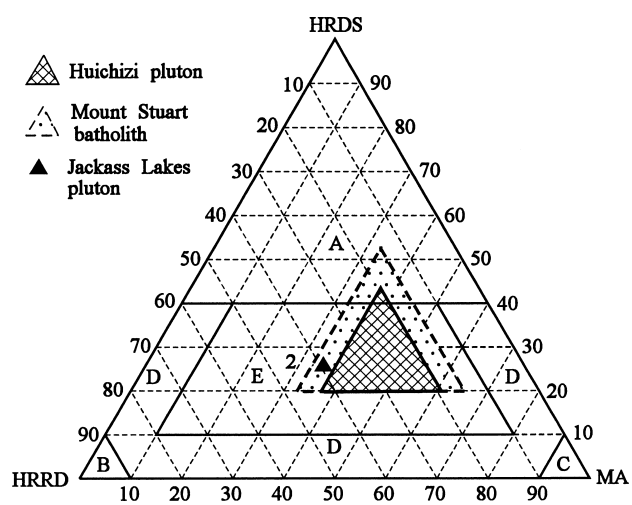

Fig. 10. Triangular diagram showing multiple emplacement mechanisms consisting of three end-member mechanisms: host-rock ductile shortening (HRDS), host-rock rigid displacement (HRRD), magmatic absorption (MA). The data of the Jackass Lakes pluton are after McNulty et al. (1996) and the Mount Stuart batholith after Paterson and Miller (1998). See the explanations in the text.

Based on the analysis given, Fig. 10 shows the three proposed mechanisms visually and quantitatively. We speculate that most granitoid plutons in nature will plot in the E field, some in the D field and few plutons in the end-member (A, B and C) fields (e.g. in-situ *S*-type granites in the C field). The Huichizi pluton is a good example showing these multiple mechanisms. In addition, two other examples are given in the E field. The Jackass Lakes pluton (McNulty et al., 1996) shows that fracture propagation (i.e. HRRD) and lateral expansion (HRDS) can account for 40% and 25% of the space needed for the pluton emplacement, respectively, the remaining 35% space was inferred to be provided by other mechanisms such as caldera building and stoping (McNulty et al., 1996), i.e. MA. For the Mount Stuart batholith (Paterson and Miller, 1998), ductile downward flow (HRDS) contributed 20–30% space; crustal thickening by folding, cleavage development, movement along reverse or fractures (HRRD) 15%; assimilation and host rock volume loss 2%, stoping (MS) 33–63% (Paterson and Miller, 1998). All these data are plotted directly in the diagram of Fig. 10, are not changed into percentage of the sum of the three end-member values. If many plutons at different times or different locations in a given region are shown in such a diagram, we believe that they will provide information on the nature of magma generation, tectonic environment and host-rock nature.

6. Conclusions

1. The Huichizi pluton features some structural patterns typical of some forceful emplacement. The fabrics in the pluton are mainly of the flattening-type ($\nu \approx 0.4$–0.9) and stronger ($Es \approx 1.0$–0.6) near the boundaries than in the center ($Es \approx 0.7$–0.3). Around the pluton, a 1.5-km-wide contact aureole is developed. Shortening in the host rock normal to the sides and ends of the pluton is 1.14 km and 0.74 km, respectively.
2. The pluton was emplaced at the present exposure level by multiple mechanisms consisting of three end-member mechanisms: (i) host-rock ductile shortening (HRDS), which produced 20% of the present-day pluton space; (ii) regional host-rock displacement, providing about 19–32% of the space; and (iii) magmatic absorption (MA), accounting for another 37% of the space. These mechanisms were active nearly simultaneously.
3. Many or most plutons in nature may be emplaced by multiple mechanisms consisting of different proportions of these three end-member mechanisms. Estimation of the magnitude of each of these mechanisms is possible and this is a valuable contribution to solving the space problem of granite emplacement.

Acknowledgements

This work was supported by the National Science Foundation of the P.R. China, Grant 49602037 and by the 1:50 000 Scale Regional Geology Survey of China. We thank Zhang Guowei, Hong Dawei, Chen Keqiang, Gao Zhenjia, Qihe Rige, Gao Bingzhang, Hu Nenggao, Jiang Changyi, Lu Xinxiang, for stimulating discussions about the pluton and we thank Xiao Qinghui, Li Shanzhong and Michael Brown for providing information about granitoid pluton research. We also wish to thank Scott R. Paterson, Zheng Yadong and Antonio Castro for careful reviewing of the manuscript and for their useful suggestions, E. Druguet and an anonymous reviewer for criticisms on the submitted manuscript.

References

Améglio, L., Vigneresse, J.L., Bouchez, J.L., 1997. Granite pluton geometry and emplacement mode inferred from combined fabric and gravity data. In: Bouchez, J.L., Hutton, D.H.W., Stephens, W.E. (Eds.), Granite: from Segregation of Melt to Emplacement Fabrics. Kluwer Academic, London, pp. 199–214.

Archanjo, C.J., Bouchez, J.L., Corsini, M., Vauchez, A., 1994. The Pombal granite pluton: magnetic fabric, emplacement and relationship with the Brasiliano strike-slip setting of NE Brazil (Paraiba State). Journal of Structural Geology 16, 323–336.

Atherton, M.P., 1993. Granite magmatism. Journal of the Geological Society of London 150, 1009–1023.

Bateman, R., 1984. On the role of deformation in the segregation, ascent and final emplacement of granitoids. Tectonophysics 10, 211–231.

Bateman, R., 1985. Aureole deformation by flattening around a diapir during in-situ ballooning: the Cannibal Creek granite. Journal of Geology 93, 293–310.

Bateman, R., 1989. Cannibal Creek granite: post-tectonic "ballooning" pluton or pre-tectonic piercement diapir? A discussion. Journal of Geology 97, 766–768.

Bouchez, L.L., Delas, C., Gleizes, A.N., Cuney, M., 1992. Submagmatic microfractures in granites. Geology 20, 35–38.

Brown, M., 1994. The generation, segregation, ascent and emplacement of granite magma: the migmatite to crustally derived granite connection in thickened orogens. Earth Science Reviews 36, 83–100.

Brun, J.P., Gapais, D., Cogne, J.P., Ledru, P., Vignerese, F.L., 1991. The Flamanville Granite (northwest France): An unequivocal example of syntectonically expanding pluton. Geological Journal 25, 271–286.

Castro, A., 1987. On granitoid emplacement and related structures: A review. Geologische Rundschau 76, 101–124.

Castro, A., Fernández, C., 1998. Granite intrusion by externally induced growth and deformation of magma reservoir, the example of the Plasenzuela pluton, Spain. Journal of Structural Geology 20, 1219–1228.

Castro, A., Moreno-ventas, I., de la Rosa, J.D., 1991. H-type (Hybrid) granitoids: a proposed revision of the granite type classification and nomenclature. Earth Science Reviews 31, 237–253.

Chappell, B.W., 1996. Magma mixing and the production of compositional variation within granite suites: evidence from the granites of southeastern Australia. Journal of Petrology 37, 449–470.

Chen, X.Z., Wang, S.R., Zhang, X.Y., 1993. Characteristics of pegmatites and the mineralization. Geology Press, Beijing (in Chinese with English abstract).

Clemens, J.D., Mawer, C.K., 1992. Granitic magma transport by fracture propagation. Tectonophysics 204, 339–360.

Collins, W.J., 1998. Evaluation of petrogenetic models for Lschlan Fold Belt granitoids: implications for crustal architecture and tectonic models. Australian Journal of Sciences 45, 483–500.

Courrioux, G., 1987. Oblique diapirism: The Criffel granodiorite/granite zoned pluton (southwest Scotland). Journal of Structural Geology 9, 313–330.

Cruden, A.R., 1990. Flow and fabric development during diapiric rise of magma. Journal of Geology 98, 681–698.

Davis, B.K., 1993. Mechanism of emplacement of the Cannibal Greek Granite with special reference to timing and deformation history of the aureole. Tectonophysics 224, 337–362.

D'Lemos, R.S., Brown, M., Strachan, R.A., 1992. The relationship between granite and shear zone: magma generation, ascent and emplacement within a transpressional orogen. Journal of the Geological Society of London 149, 487–490.

Dunnet, D., 1969. A technique of finite strain analysis using elliptical particles. Tectonophysics 7, 117–136.

Faure, G., 1986. Principles of Isotopic Geology, 2nd ed. John Wiley, New York.

Fowler T.K. Jr, Paterson, S.R., 1997. Timing and magmatic fabric form structural relations around stoped blocks. Journal of Structural Geology 19, 209–224.

Fowler T.K. Jr, Paterson, S.R., Crossland, A., Yoshinobu, A., 1995. Pluton emplacement mechanisms: a view from the roof. In: Brown, M., Piccoli, P.M. (Eds.), The Origin of Granites and Related Rocks: Third Hutton Symposium Abstracts, U.S. Geological Survey Circular 1129, p. 57.

Glazner, A.F., 1991. Plutonism, oblique subduction and continental growth: An example from the Mesozoic of California. Geology 19, 784–786.

Godin, P., 1994. Deformation within the Cannibal Creek Pluton and its aureole, Queensland, Australia: a reevaluation of ballooning as an emplacement mechanism. Journal of Structural Geology 16, 693–708.

Grocott, J., Brown, M., Dallmeyer, R.D., Taylor, G.K., Treloar, P.J., 1994. Mechanisms of continental growth in extensional arcs: An example from the Andean plate boundary zone. Geology 22, 391–394.

Guglielmo G. Jr, 1993. Magmatic strains and foliation triple points of the Merrimac plutons, northern Sierra Nevada, California: implications for pluton emplacement and timing of subduction. Journal of Structural Geology 15, 177–189.

Guglielmo G. Jr, 1994. Interference between pluton expansion and coaxial tectonic deformation: three-dimensional computer model and field implications. Journal of Structural Geology 16, 237–252.

Guineberteau, B., Bouchez, J.L., Vigneresse, J.L., 1987. The Mortagne granite pluton (France) emplaced by pull-apart along a shear zone. Structural and gravimetric arguments and regional implications. Geological Society of America Bulletin 99, 763–770.

Hecht, L., Vigneresse, J.L., Morteani, G., 1997. Constraints on the origin of zonation of the granite complex in the Fichtelgebirge (Germany and Czech Republic): evidence from a gravity and geochemical study. Geologische Rundschau 86 (Suppl.), 93–109.

Hsu, T.C., 1966. The characteristics of coaxial and non-coaxial strain path. Journal of Strain Analysis 1, 216–222.

Hutton, D.H.W., 1982. A tectonic model for the emplacement of the Main Donegal granite, NW Ireland. Journal of Geological Society, London 139, 615–631.

Hutton, D.H.W., 1988a. Granite emplacement mechanisms and tectonic controls: Inferences from deformation studies. Royal Society of Edinburgh Transactions. Earth Sciences 79, 245–255.

Hutton, D.H.W., 1988b. Igneous emplacement in shear zone termination: The biotite granite at Strontian, Scotland. Geological Society of America Bulletin 100, 1392–1399.

Hutton, D.H.W., 1992. Granite sheeted complexes: Evidence for the dyking ascent mechanism. Royal Society of Edinburgh Transactions. Earth Sciences 83, 377–382.

Hutton, D.H.W., 1997. Syntectonic granites and the principle of effective stress: A general solution to the space problem? In: Bouchez, J.L., Hutton, D.H.W., Stephens, W.E. (Eds.), Granite: from Segregation of Melt to Emplacement Fabrics. Kluwer Academic, London, pp. 189–197.

Hutton, D.H.W., Reavy, R.J., 1992. Strike-slip tectonics and granite petrogenesis. Tectonics 11, 960–967.

Hutton, D.H.W., Dempster, T.J., Brown, P.E., 1990. A new mechanism of granite emplacement: Intrusion in active extensional shear zones. Nature 343, 452–455.

John, B.E., Blundy, J.D., 1993. Emplacement-related deformation of granitoid magmas, southern Adamello massif, Italy. Geological Society of America Bulletin 105, 1517–1541.

Karlstrom, K.E., Miler, C.F., Kingsbury, J.A., Wooden, J.L., 1993. Pluton emplacement along an active ductile thrust zone, Piute Mountains, southeastern California: Interaction between deformational and solidification processes. Geological Society of America Bulletin 105, 213–230.

Keay, S., Collins, W.J., McCulloch, M.T., 1997. A three-component mixing model for granitoid genesis: Lachlan Fold Belt, eastern Australia. Geology 25, 307–310.

Law, R.D., Morgan, S.S., Casey, M., Sylvester, A.G., Nyman, M., 1992. The Papoose Flat pluton of eastern Californian: A reassessment of its emplacement history in the light of new microstructural and crystallographic fabric orientations. Royal Society of Edinburgh Transactions. Earth Sciences 83, 361–376.

Leek, S.E., 1990. Granite magma, their sources, initiation and consequences of emplacement. Journal of the Geological Society of London 147, 579–589.

Lerch, M.F., Xue, F., Krǒner, A., Zhang, G.W., Todt, W., 1995. A middle Silurian–Early Devonian magmatic arc in the Qinling Mountains of Central China. Journal of Geology 103, 437–449.

Li, W.P., Wang, T., 1995a. Lithodemic units of granitoid rocks of the Huichizi complex intrusion in the eastern Qinling and its geological significance, central China. Regional Geology of China 53, 136–141 (in Chinese with English abstract).

Li, W.P., Wang, T., 1995b. Geologic feature and genesis of the Huichizi complex pluton in the eastern Qinling, central China. Journal of Mineralogy and Petrology 5, 8–15 (in Chinese with English abstract).

Li, W.P., Wang, T., 1999. Estimation of the proportion of mantle-derived magma to crustal-derived magma in the Huichizi complex pluton, eastern Qinling, central China. Earth Science, Acta Petrological Sinica, in press (in Chinese with English abstract).

Mahmood, A., 1985. Emplacement of the Zaer pluton, Morocco. Geological Society of America Bulletin 96, 931–939.

Marre, J., 1986. The Structural Analysis of Granitic Rocks. Elsevier, Amsterdam.

Marsh, B.D., 1982. On the mechanics of igneous diapirism, stoping and zone melting. American Journal of Science 282, 808–855.

McCaffrey, K.J., Petford, N., 1997. Are granitic intrusions scale invariant? Journal of the Geological Society of London 154, 1–4.

McNulty, B.A., Tong, W., Tobisch, O.T., 1996. Assembly of a dike-fed magma chamber: The Jackass Lakes pluton, central Sierra

Nevada, California. Geological Society of America Bulletin 108, 926–940.

Miller, R.B., Paterson, S.R., 1994. The transition from magmatic to high-temperature solid-state deformation: implications from the Mount Stuart batholith, Washington. Journal of Structural Geology 16, 853–865.

Paterson, S.R., Fowler T.K. Jr, 1993a. Re-examining pluton emplacement process. Journal of Structural Geology 15, 191–206.

Paterson, S.R., Fowler T.K. Jr, 1993b. Extensional pluton emplacement models: Do they work for the large plutonic complexes. Geology 21, 781–784.

Paterson, S.R., Miller, R.B., 1998. Magma emplacement during arc-perpendicular shortening: An example from the Cascades crystalline core, Washington. Tectonics 17, 571–586.

Paterson, S.R., Fowler T.K. Jr, Schmidt, K.L., Yoshinobu, A.S., Yuan, E.S., Miller, R.B., 1998. Interpreting magmatic fabric patterns in plutons. Lithos 48, 53–82.

Paterson, S.R., Vernon, R.H., 1995. Bursting the bubble of ballooning plutons: A return to nested diapirs emplaced by multiple process. Geological Society of America Bulletin 107, 1356–1380.

Paterson, S.R., Fowler T.K. Jr, Miller, R.B., 1995. Pluton emplacement in arcs: a crustal-scale recycling process. In: Brown, M., Piccoli, P.M. (Eds.), The Origin of Granites and Related Rocks: Third Hutton Symposium Abstract, U.S. Geological Survey Circular 1129, pp. 111–112.

Paterson, S.R., Vernon, R.H., Tobisch, O.T., 1989. A review of the criteria for the identification of magmatic and tectonic foliations. Journal of Structural Geology 11, 349–363.

Petford, M., Atherton, M.P., 1992. Granitoid emplacement and deformation along a major crustal lineament: the Cordillera Blanca, Peru. Tectonophysics 205, 171–185.

Pitcher, W.S., 1979. The nature, ascent and emplacement of granite magma. Journal of the Geological Society of London 136, 617–662.

Ramsay, J.G., 1989. Emplacement kinematics of a granite diapir: The Chinadamora batholith, Zimbabwe. Journal of Structural Geology 11, 190–210.

Royden, L.H., 1993. The tectonic expression of slab pull at continent convergent boundaries. Tectonics 12, 303–325.

Saleeby, J.B., 1991. The Cretaceous Sierra Nevada—A trans-sitiching batholithic belt. Geological Society of America Abstracts with Programs 23, 94.

Sanderson, D.J., Meneilly, A.W., 1981. Analysis of three-dimensional strain modified uniform distribution: andalusite fabrics from a granite aureole. Journal of Structural Geology 3, 1909–1916.

Schwerdtner, S.M., 1995. Local displacement of diapir contacts and its importance to pluton emplacement study. Journal of Structural Geology 17, 909–910.

Shang, W.J., Yan, Z., 1988. Granites in Shaangxi Province, China. Northwest University Press, Xi'an (in Chinese with English abstract).

Siebel, W., Trezeski, R., Stettner, G., Hecht, L., Casten, U., Hohndorf, A., Muller, P., 1997. Granite magmatism of the NW Bohemian massif revealed: gravity data, composition, age relation and phase concept. Geologische Rundschau 86 (Suppl.), 45–63.

Sylvester, A.G., Oertel, G., Nelson, C.A., Christie, J.M., 1978. Papoose Flat pluton: a granite blister in the Inyo Mountain, Californian. Geological Society of America Bulletin 89, 1205–1219.

Thompson, A.B., Schulmann, K., Jezek, J., 1997. Extrusion tectonics and elevation of lower crustal metamorphic rocks in convergent orogens. Geology 25, 491–494.

Trzebski, R., Behr, H.J., Conrad, W., 1997. Subsurface distribution and tectonic setting of the late-Variscan granite in the northwestern Bohemian Massif. Geologische Rundschau 86 (Suppl.), 64–78.

Tobisch, O.T., Cruden, A.R., 1995. Fracture-controlled magma conduits in an obliquely convergent continental magmatic arc. Geology 23, 941–944.

Van den Eeckhout, B., Grocott, J., Vissers, R., 1986. On the role of diapirism in the segregation, ascent and final emplacement of granitoid magma—Discussion. Tectonophysics 127, 161–169.

Vernon, R.H., Paterson, S.K., 1993. The Ardara granite Ireland: Deflating an expand intrusion. Lithos 31, 17–31.

Wang, T., 1988. A method of computer simulation diagram of Dunnet's strain measurement method. A Selection of Papers of Young Geologists. Northwest University Press, Xi'an (in Chinese with English abstract).

Wang, T., Li, W.P., 1996. 1:50000 Regional Geological Surveys of I49E01402 (Shiziping), P. R. China (in Chinese).

Wang, T., Hu, N.G., Yan, G.X., Li, W.P., 1995. The characteristics of deformation, metamorphism and the evolution of Qinling group in the Eastern Qinling. Journal of Geotectonics 5, 11–18 (in Chinese with English abstract).

Wang, T., Hu, N.G., Pei, X.Z., Li, W.P., 1997a. The composition, structural regime and evolution of the core complex of the Qinling orogenic belt, central China. Acta Geoscientia Sinica 18, 345–351 (in Chinese with English abstract).

Wang, T., Hu, N.G., Pei, X.Z., Li, W.P., 1997b. Lateral westward motion of the core complex of the Qinling orogenic belt, central China. Scientia Geologica Sinica 32, 423–431 (in Chinese with English abstract).

Wang, T., Wang, X.X., Li, W.P., 1997c. The development mechanism of the foliation of the Huichizi granite pluton in the Qinling complex, central China. Journal of Geotectonics 6, 10–16 (in Chinese with English abstract).

Weinberg, R.F., 1995. Diapirism of crustal magma. In: Brown, M., Piccoli, P.M. (Eds.), The Origin of Granites and Related Rocks: Third Hutton Symposium Abstract, U.S. Geological Survey Circular 1129, pp. 161–162.

Weinberg, R.F., Podladchikov, Y., 1994. Diapiric ascent of magmas through power law crust and mantle. Journal of Geophysical Research 99, 9543–9560.

Yoshinobu, A.S., Okaya, D.A., Paterson, R.R., Fowler T.K. Jr, 1995. Testing fault controlled magma emplacement mechanisms. In: Brown, M., Piccoli, P.M. (Eds.), The Origin of Granites and Related Rocks: Third Hutton Symposium Abstract, U.S. Geological Survey Circular 1129, p. 166.

You, Z.D., Suo, S.T., 1991. Metamorphic process and structural analysis of the core complex of an orogenic belt: example from the Eastern Qinling Mountain. China University of Geosciences Press (in Chinese with English abstract).

You, Z.D., Suo, S.T., Han, Y.Q., Zhong, Z.Q., Chen, N.S., 1990. The major characteristics of the metamorphic complex of the Qinling orogenic belt and their implications for the construction of the eastern Qinling continental crust. In: Ye, L.J., Qian, X.Z., Zhang, G.W. (Eds.), A Selection of Papers Presented at the Conference on the Qinling Orogenic Belt. Northwest University Press, Xi'an, pp. 1–14 (in Chinese with English abstract).

Yuan, X., 1991. Deep structure and tectonic evolution of Qinling orogenic belt, central China. In: Ye, L.J., Qian, X.L., Zhang, G.W. (Eds.), A Selection of Papers Presented at the Conference on the Qinling Orogenic belt. Northwest University Press, Xi'an, pp. 174–184 (in Chinese with English abstract).

Zhang, H.F., Zhang, B.R., Luo, T.S., 1994. Discussion on the source of the materials of the Huichizi granite pluton in northern Qinling, China. Journal of Mineralogy and Petrology 1, 67–73 (in Chinese with English abstract).

Zhang, G.W., Zhou, D.W., Sun, Y., Xue, F., Zhang, C.L., 1988. The composition deformation and metamorphism of the Qinling complex in the Qinling Mouniains. In: Zhang, G.W. (Ed.), Formation and Evolution of the Qinling Mountains. Northwest University Press, Xi'an, pp. 99–114 (in Chinese with English abstract).

Zhang, G.W., Yu, Z.P., Sun, Y., Cheng, S.Y., Li, T.H., Xue, F., Zhang, C.L., 1989. The major suture zone of the Qinling orogenic belt. Journal of Southeast Asian Earth Sciences 3, 63–76.
Zhang, G.W., Xiang, L., Men, Q.R., 1995a. The Qinling orogen and intercontinental orogen mechanisms. Episodes 8, 36–39.
Zhang, G.W., Zhang, Z.Q., Dong, Y.P., 1995b. Nature of main tectono-lithostratigraphic units of the Qinling orogen: Implication for the tectonic evolution. Acta Petrological Sinica 11, 101–114 (in Chinese with English abstract).
Zhang, H.F., Zho, Z.D., Luo, T.C., Zhang, B.R., 1995. Crustal growth and lower crust nature of North Qinling: study of Sm–Nd istopic model ages. Acta Petrological Sinica 2, 160–170 (in Chinese with English abstract).
Zhang, H.F., Zhang, B.R., Luo, T.C., 1996. The source features of the Piaochi granite pluton and its tectonic setting, north Qinling. Geological Review 42, 209–214 (in Chinese with English abstract).
Zulauf, G., Maier, M., Stocknert, B., 1997. Depth of intrusion and thermal modeling of the Falkenberg granite (Oberpfalz, Germany). Geologische Rundschau 86 (Suppl.), 64–78.